JOURNAL OF CATALYSIS 132, 490–497 (1991)

Titania-Supported Bimetallic Catalyst Synthesis by Photocatalytic Codeposition at Ambient Temperature: Preparation and Characterization of Pt–Rh, Ag–Rh, and Pt–Pd Couples

JEAN-MARIE HERRMANN,[1,*] JEAN DISDIER,* PIERRE PICHAT,* ASUNCIÓN FERNÁNDEZ,† AGUSTÍN GONZÁLEZ-ELIPE,† GUILLERMO MUNUERA, AND CHRISTIANE LECLERCQ‡

**URA au CNRS "Photocatalyse, Catalyse et Environnement," Ecole Centrale de Lyon, BP 163, 69131 Ecully Cédex, France; †Instituto de Ciencia de Materiales and Departamento de Química Inorgánica, Centro Mixto CSIC, Universidad de Sevilla, Aptdo 1115, 41071 Sevilla, Spain; and ‡Institut de Recherches sur la Catalyse, CNRS, 69626 Villeurbanne Cédex, France*

Received April 8, 1991; revised July 30, 1991

We have examined the possibilities of preparing some bimetallic catalysts supported on TiO_2 (Degussa P-25) by UV illumination ($\lambda > 300$ nm, radiant flux, 60 mW cm^{-2}), at room temperature for 24 h, of aqueous suspensions containing 500 mg of this oxide, and cations of the desired metals in amounts corresponding to metal loadings between 0.5 and 2.5 wt% if complete reduction were achieved. In the case of the H_2PtCl_6–$RhCl_3$ couple, Rh deposition almost did not take place. For the mixture $AgNO_3$–$RhCl_3$ at pH 2.6, Rh deposition was substantial but still incomplete. In contrast, Rh deposition was complete in aqueous ammonia (pH 11). TEM and STEM–EDX analysis of the solid recovered in this latter case showed that Rh formed 1- to 3-nm particles and was also found in 8- to 30-nm particles containing ca. 80 wt% Ag (with respect to Rh) presumably as a result of its deposition on more rapidly crystallized Ag. Solids prepared from H_2PtCl_6 and $Pd(NO_3)_2$ were studied in more detail because both metals were completely deposited, at least at levels ≤ 1 wt%. They were heterogeneous, since Pd and Pt formed ca. 1- or 3-nm crystallites, respectively; however, most of the crystallites were found to contain both metals with a high and varied proportion of Pd. An XPS Ar^+-sputtering depth profile of the 1 wt% Pt–1 wt% Pd/TiO_2 sample showed a similar behavior for Pt and Pd, which might indicate the formation of a solid solution in some particles. As this formation is attributed to similar reduction rates for both metallic salts, it is inferred that alloys are obtained only in cases where the salts and conditions can be chosen to fulfill this requirement. This limits the capabilities of the photoassisted codeposition method for preparing effective bimetallic supported catalysts.

INTRODUCTION

When a photosensitive semiconductor is irradiated in the presence of a noble metal salt or complex with photons of suitable energy ($h \geq$ Eg: band gap energy), the metal can be deposited as small crystallites. This phenomenon has been known for about 25 years (*1*, *2*) but has only been systematically investigated over the last few years. The metals used have been Pt (*3–10*), Pd (*8–18*), Rh (*8*, *9*), Au (*9*, *19*, *20*), Ir (*10*), and Ag (*1*, *2*, *21–27*). They were deposited on various semiconductors, mainly oxides such as ZnO, WO_3, and predominantly TiO_2. Photosensitive sulfides such as CdS can also be used (*10*). The photocatalytic deposition has been employed as a means of preparing metal-supported catalysts (*5*, *6*, *10*, *13*, *14*) or photocatalysts (*5*) and as a potential method of metal recovery from aqueous effluents (*8*, *9*, *19*, *20*, *27*, *28*).

Several monometallic catalysts have thus been prepared and the codeposition by the same technique of two metals was suggested as a possible method for the synthesis of bimetallic catalysts (*9*, *10*). However, investigations are necessary to check the validity of this suggestion. They include the study of different metallic couples, loadings, and

---

[1] To whom correspondence should be addressed.

0021-9517/91 $3.00

TABLE 1

Metal Loadings Obtained during the Photocatalytic Codeposition of Noble Metals on TiO_2 (500 mg TiO_2, Illumination Time, 24 h; Radiant Flux, 60 mW cm^{-2}, $\geq$300 nm).

Couple	Metal	wt% Desired	wt% Obtained
Rh–Pt	Rh	2.5	0.05
	Pt	2.5	1.4
Rh–Ag	Rh	1.0	0.6
	Ag	1.0	1.0
Pt–Pd	Pt	0.5	0.5
	Pd	0.5	0.5
	Pt	1.0	1.0
	Pd	1.0	1.0
	Pt	2.0	1.5
	Pd	2.0	1.9

especially the effects of various parameters and conditions.

In this paper, we present the photocatalytic codeposition on TiO_2 of three different couples: Pt–Rh, Ag–Rh, and Pt–Pd. The Pt–Pd and Pt–Rh couples are of interest because of their potential application in auto-exhaust catalysts (*29*), whereas the significance of the Ag–Rh couple is only academic. TiO_2 was chosen because of its efficiency in this method. The TiO_2 Degussa P-25 sample used here is commonly employed in photocatalytic processes for its especially high efficiency.

Contrary to most previous studies, the data presented here include not only the percentages deposited for each metal but also an examination of the metal particles by various surface analysis techniques, conducted particularly to determine whether alloys are formed.

EXPERIMENTAL

Materials

TiO_2 was Degussa P-25 (50 $m^2 g^{-1}$, nonporous, ca. 70% anatase). Pure-grade reagents were purchased either from Merck (H_2PtCl_6, $RhCl_3$, and $AgNO_3$) or from Ventron ($Pd(NO_3)_2$).

Photoreactor

The photodepositions were carried out in a Pyrex flask of 100-cm^3 vol equipped with an optical window of the same material transparent to wavelengths >300 nm. UV light was provided by a Philips HPK 125 W mercury lamp. The radiant flux measured with a radiometer (United Detector Technology Model 21 A) was 60 mW cm^{-2}.

Procedure

The slurry containing 500 mg TiO_2 in 40 cm^3 of the solution was stirred under pumping for 2 min to remove air. After a second pumping following a period of 15 min of stirring under static vacuum, the photoreactor was oxygen-free according to the chromatographic analysis. The subsequent illumination was carried out for 24 h. The metal-deposited samples were then separated by centrifugation and dried at 383 K in air for 10 h.

Analysis

The concentration of the cations remaining in the solution after illumination was measured by atomic absorption spectroscopy.

X-ray photoelectron spectroscopy (XPS) spectra were recorded with a Leybold–Her-

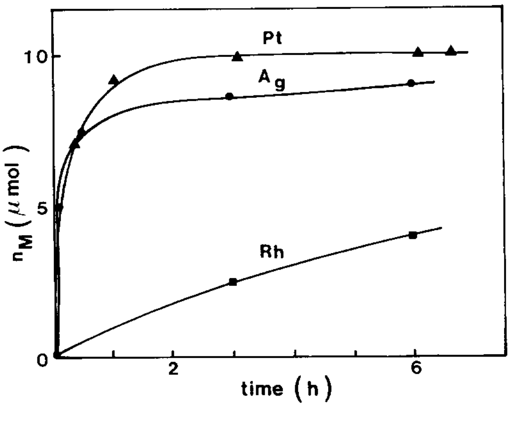

FIG. 1. Comparative photodeposition rates of Ag, Pt, and Rh on titania in separate experiments under identical conditions (m_{TiO_2} = 70 mg; V = 10 cm^3 of 10^{-3} *M* solution of Ag NO_3, H_2PtCl_6 or $RhCl_3$).

TABLE 2

Atomic Percentages Derived from XPS Analysis of the M–M'/TiO_2 samples

Sample	0	Ti	M	M'
Pt–Rh/TiO_2	66.9	32.6	0.5(Pt)	n.m.(Rh)
Ag–Rh/TiO_2	67.8	31.8	0.1(Ag)	0.3(Rh)
Pt–Pd/TiO_2 (1.0 wt% Pt–1.0 wt% Pd)	69.5	29.5	0.5(Pt)	0.5(Pd)
Pt–Pd/TiO_2 (1.5 wt% Pt–1.9 wt% Pd)	67.8	30.7	0.5(Pt)	1.0(Pd)

Note. n.m., not measurable.

aeus LHS-10 spectrometer using Mg$K\alpha$ radiation as the excitation source (1253.6 eV) and a pass energy of 50 eV. The binding energy (B.E.) reference was taken at the Ti $2p^{3/2}$ level of Ti^{4+} at 458.5 eV. Ion sputtering was carried out by means of a Peening ionization source supplied with argon and operated at an accelerating voltage of 3.5 keV. Area calculations were made on line with the spectrometer by use of a HP-1000E computer. Sensitivity factors, supplied with the instrument, were employed to calculate the atomic percentages.

Transmission electron microscopy (TEM) examinations were performed with a JEOL 100C microscope and STEM–EDX analyses were performed with a STEM field-emission gun (VGHB 501) equipped with a silicon–lithium diode detector (Link) and a multichannel analyzer (Tracor 5500). The samples were dispersed by sonication in ethanol and deposited on a carbon film supported on a copper grid responsible for the Cu signals in the EDX analysis spectra (Figs. 2 and 3).

RESULTS AND DISCUSSION

Previous Results on the Photocatalytic Deposition of Various Noble Metals on Titania

Under the conditions used in an earlier report (*10*) (50 mg TiO_2 in 10 cm^3 10^{-3} M metal salt solution, t_{UV} = 1 h), the reactivity pattern that resulted was

$$\mathrm{Ag} > \mathrm{Pd} > \mathrm{Au} > \mathrm{Pt} \gg \mathrm{Rh} \gg \mathrm{Ir} \gg \mathrm{Cu} \simeq \mathrm{Ni} = 0$$

SCHEME 1

The corresponding metal salts or complexes used were $AgNO_3$, $PdCl_2$, $AuCl_3$, H_2PtCl_6 (or Na_2PtCl_6), $RhCl_3$, H_2IrCl_6, $Cu(NO_3)_2$, and $Ni(NO_3)_2$.

The photodeposition of all the metals presently studied is thermodynamically possible since the redox potentials of the metal or complex ions are in a favorable position with respect to the flat band potential of titania as discussed in Refs. (*8, 9*). Moreover, the photodeposition of these metals does not need an electron-donor reagent since the electron transfer from the surface of titania to the metal ion or complex is spontaneous according to the favorable redox potential mentioned above.

1. Photocodeposition of platinum and rhodium. For the photocodeposition of Pt and Rh, an aqueous mixture of H_2PtCl_6 and $RhCl_3$ at pH 2 was used. The quantities were calculated to obtain deposits corresponding to 2.5 wt% for each metal. In fact, very reproducible results showed that the weight percentage of deposited Pt was 1.4 and that of Rh 0.05 only (Table 1). The quasi-absence of Rh deposition is consistent with its slow photodeposition rate as compared with that of platinum under the experimental conditions indicated in Fig. 1. However, an inhibition of the Rh photoreduction as a result of the presence of H_2PtCl_6 should intervene since rhodium can be photodeposited on a Pt/TiO_2 sample (*9, 30*). Accordingly, Pt–Rh/TiO_2 catalysts cannot be prepared by photocodeposition, at least under these conditions.

TEM examination revealed the presence of metal particles of ca. 1–1.5 nm on most regions of the oxide support with, however, some areas carrying a greater number of metal particles. XPS spectroscopy revealed that platinum was essentially present as Pt^{2+} species. These species were completely reduced to Pt° by treatment in a hydrogen atmosphere (10 Torr) at 473 K for 1 h. The hydro-

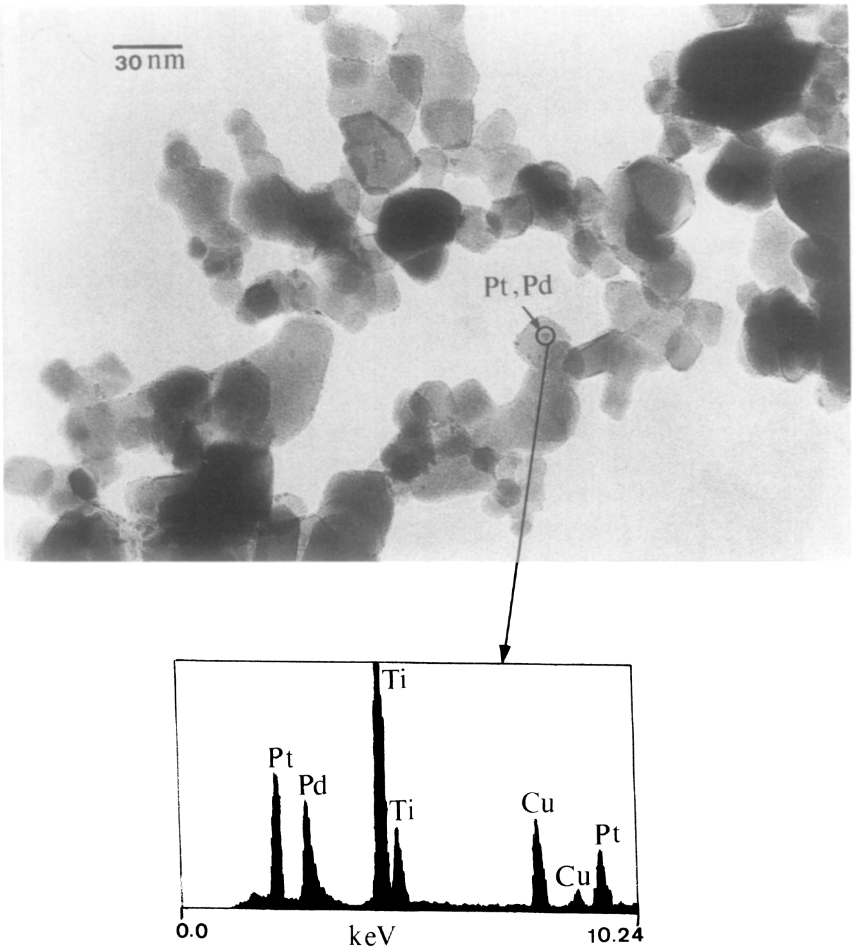

FIG. 2. TEM micrograph of the 1 wt% Pt–1 wt% Pd/TiO_2 sample and STEM–EDX analysis of a bimetallic particle.

gen treatment also removed chlorine ions as shown by XPS analysis of this element.

2. Photocodeposition of silver and rhodium. For the photocodeposition of silver and rhodium, an aqueous mixture of $AgNO_3$ and $RhCl_3$ at pH 2.6 was used. The quantities were calculated to obtain 1 wt% deposits of each metal. Highly reproducible results showed that silver was completely deposited, while ca. 40% of the rhodium cations remained in the solution. Here again, the incomplete photodeposition of Rh can be attributed to its slower rate of reduction (Fig. 1). XPS analyses of both metals are given in Table 2. The low intensity of the Ag XPS peak reflects the low dispersion (particles of 8–30 nm in diameter as shown by TEM, in agreement with previous results for the photodeposition of Ag alone (*27*)). XPS analysis also showed that rhodium is mainly present as Rh^{3+} ions as expected from the aerial chemisorption of oxygen during storage according to the stoichiometry (*31*):

$$2\ Rh_s + \tfrac{3}{2}\ O_2(g) \rightarrow 2\ Rh_2O_3.$$

These Rh^{3+} species are reduced to Rh° atoms by a H_2 treatment (P_{H_2} = 10 Torr) at 473 K for 1 h (1 Torr = 133.3 Pa).

The photocodeposition of Ag and Rh on titania was also carried out at pH 11, which

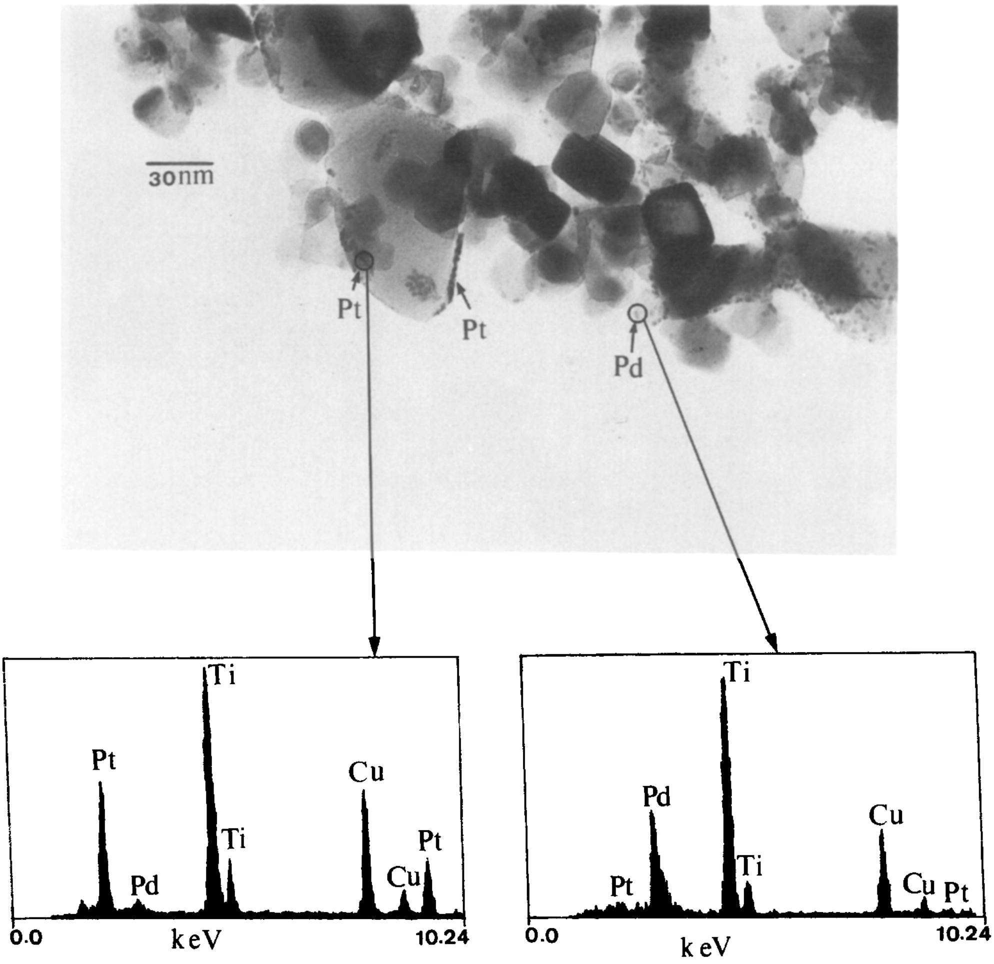

FIG. 3. TEM micrograph of the 1.5 wt% Pt–1.9 wt% Pd/TiO_2 sample and STEM–EDX analysis of two types of particles.

was obtained with an aqueous solution of ammonia. It was complete for both metals. TEM and STEM studies revealed two kinds of metal particles: (i) rhodium particles (1–3 nm in diam) occasionally concentrated on some areas of the support and (ii) 8- to 30-nm-diameter particles, containing ca. 80 wt% Ag. The formation of these latter particles can be explained by the deposition of Rh on the Ag particles previously formed because of their greater rate of deposition (Scheme 1 and Fig. 1). This location is favored by the alkaline medium as found previously for the photodeposition of Rh on Pt/TiO_2 catalysts (*30*). These bimetallic particles do not constitute alloys since the photodeposition is sequential. Consequently, they are not of interest for catalysis but might be considered for other applications, for instance in the field of material science.

3. Photocodeposition of platinum and palladium. For the photocodeposition of Pt and Pd, an aqueous solution of H_2PtCl_6 and $Pd(NO_3)_2$ was used at pH 1.9. The quantities were calculated to obtain deposits corresponding to three different loadings: 0.5, 1.0, and 2.0 (in wt%) for each metal. The photodeposition was complete for both metals in the case of the two lower contents, whereas only 1.5 wt% Pt and 1.9 wt% Pd

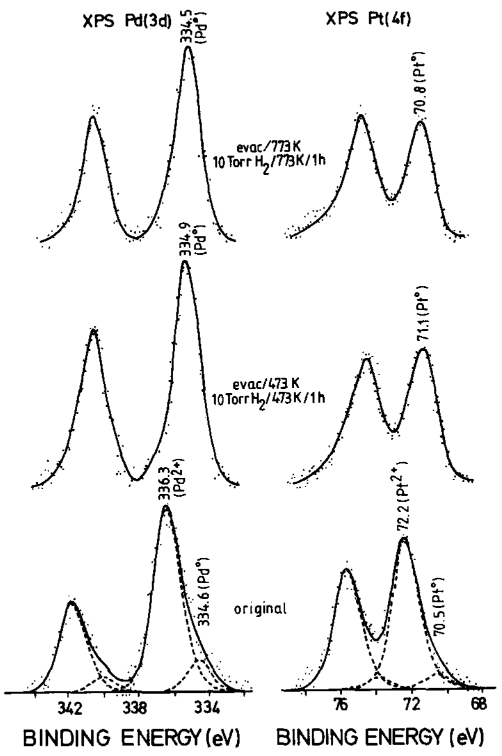

FIG. 4. XPS analysis of the 1 wt% Pt–1 wt% Pd/TiO_2 sample. The treatments are indicated in the central part of the figure.

were obtained in the third case (Table 1). It should be emphasized that these results refer to specific conditions. At other pH and illumination time, they would have been different.

TEM examination indicated that metal particles were distributed on all the grains of the support, although, as expected, the metal particle distribution was better for the samples with smaller contents ($\leq$1 wt%) (Fig. 2). However, even in that case, some regions of the support could be found with a higher density of metal particles. The diameter of the majority of the particles was ca. 1 nm. Some bigger particles of ca. 3 nm in diameter were also present but they were much less numerous and their number was smaller the lower the metal percentage. STEM–EDX analysis of the 1 wt% Pt–1 wt% Pd/TiO_2 sample indicated the existence of three types of metal particles: (i) the ca. 1-nm crystallites were principally constituted by palladium but some of them also contained platinum; (ii) some ca. 3-nm particles were formed of platinum; and (iii) most of the ca. 3-nm particles contained both palladium and platinum (Fig. 2), with percentages varying from 50 wt% Pd–50 wt% Pt to 80 wt% Pd–20 wt% Pt; i.e., palladium was always more abundant than platinum. The predominance of Pd could be due to a slightly higher initial rate of photodeposition of this metal. The weight difference in platinum with respect to the nominal content could be accounted for by the existence of larger Pt particles (3 nm) as indicated above. The presence of bimetallic particles enables one to envisage the existence of a Pd–Pt alloy.

Although STEM examination of the 0.5 wt% Pd–0.5 wt% Pt/TiO_2 sample was close to the detection limit, it provided similar results, qualitatively.

The 1.5 wt% Pt–1.9 wt% Pd/TiO_2 sample was more heterogeneous, with platinum particles sometimes agglomerated at TiO_2 grain boundaries, as is clearly visible in the micrograph of Fig. 3.

XPS analyses were carried out on the 1 wt% Pt–1 wt% Pd/TiO_2 sample (Fig. 4). They indicated that Pt and Pd are mainly present as Pt^{2+} and Pd^{2+} ions in agreement with previous results (*4*). In our opinion, this does not mean that the photoreduction of Pt^{IV} is limited to the +2 level, as suggested in Ref. (*4*), but to results from the chemisorption of ambient oxygen during the storage. Chemisorbed oxygen can be removed in a hydrogen atmosphere at 473 K (Fig. 4). Treatment in 10 Torr H_2 at 773 K for 1 h produces a decrease of the binding energy of Pt and Pd in agreement with the occurrence of the so-called "Strong metal-support interaction (SMSI) effect" observed with metal catalysts prepared by impregnation and chemical reduction.

The XPS analysis was completed by carrying out an Ar^+-sputtering depth profile. A model has been proposed (*32*) describing the

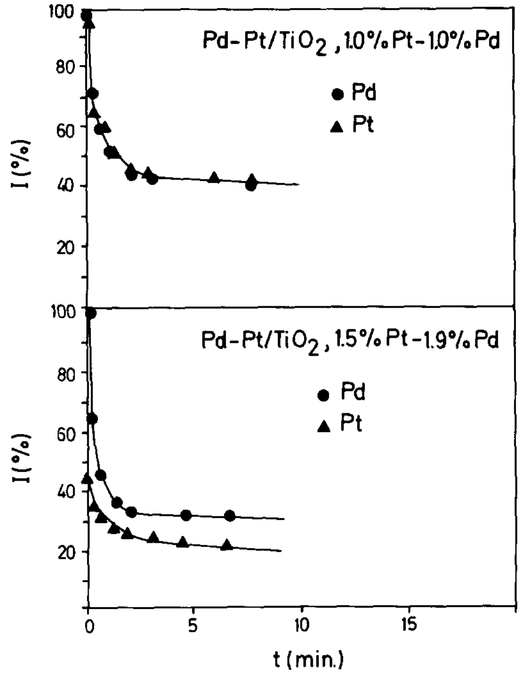

FIG. 5. Ar$^+$ sputtering: comparative XPS analysis of the depth profiles of the 1 wt% Pt–1 wt% Pd/TiO$_2$ and the 1.5 wt% Pt–1.9 wt% Pd/TiO$_2$ photodeposited samples.

sputtering behavior of catalysts or of any other powder formed by a carrier and a dispersed phase supported on it. According to that model, the shape of the sputtering profiles of the dispersed phase should provide some semiquantitative information on the average particle size and the formation of a solid solution. The depth profile of the 1 wt% Pt–1 wt% Pd/TiO$_2$ sample (Fig. 5) shows identical behavior of both metals, which demonstrates that one metal does not cover the other and is in favor of a homogeneous bimetallic solid with a reasonably high probability of the presence of a Pt–Pd alloy in most of the particles, according to the STEM analysis previously described. By contrast, for the 1.5 wt% Pt–1.9 wt% Pd/TiO$_2$ sample, the relative intensity of the palladium signal decreases more abruptly than that of platinum. This reflects a more heterogeneous catalyst with crystallites of palladium that are smaller than those of platinum and consequently more sensitive to Ar$^+$ sputtering.

CONCLUSION

The results of the three cases tested can consistently be interpreted on the basis of the reduction rates of the metallic cations considered (Scheme 1). Successive reductions obviously cannot produce bimetallic solid solutions. Furthermore, the reduction of rhodium was found inhibited by the presence of platinum or silver cations. In addition, even in the favorable cases of not too different reduction rates, the Pt–Pd/TiO$_2$ example shows that an acceptable distribution of small metal particles is likely to be obtained only for contents ≤ 1 wt% as a result of the agglomeration of crystallites in concentrated solutions or under prolonged UV illumination in diluted solutions; note, however, that these low contents are usually employed for most catalytic processes. This study also indicates that the design of an effective Pt–Pd/TiO$_2$ catalyst by this method would require further studies to determine more precisely the effects of various metallic salts or complexes and of various photoassisted deposition conditions to discover those that achieve similar rates of reduction and, accordingly, deposition.

ACKNOWLEDGMENTS

The authors thank the Commission of the European Communities (CEC) (Stimulation Action, Contract ST2J0474) and the "Junta de Andalucía" for financial support.

REFERENCES

1. Clark, W. C., and Vondjidis, A. G., *J. Catal.* **4**, 691 (1965).
2. Korsunovskii, G. A., *Russ. J. Phys. Chem.* **39**, 1139 (1965).
3. Krauetler, B., and Bard, A. J., *J. Am. Chem. Soc.* **100**, 4317 (1978).
4. Sungbom, C., Kawai, M., and Tanaka, K., *Bull. Chem. Soc. Jpn.* **57**, 871 (1984).
5. Sato, S., *J. Catal.* **92**, 11 (1985).
6. Nakamatsu, H., Kawai, T., Koreeda, A., and Kawai, S., *J. Chem. Soc., Faraday Trans. 1* **82**, 527 (1985).

7. Koudelka, M., Sanchez, J., and Augustynski, J., *J. Phys. Chem.* **86,** 4277 (1982).
8. Herrmann, J. M., Disdier, J., and Pichat, P., *J. Phys. Chem.* **90,** 6028 (1986).
9. Borgarello, E., Serpone, N., Emo, G., Harris, R., Pelizzetti, E., and Minero, C., *Inorg. Chem.* **25,** 4499 (1986).
10. Herrmann, J. M., Disdier, J., Pichat, P., and Leclercq, C., *in* "Preparation of Catalysts IV" (B. Delmon, P. Grange, P. A. Jacobs, and G. Poncelet, Eds.), p. 285. Elsevier, Amsterdam, 1987.
11. Möllers, F., Tolle, H. J., and Memming, R., *J. Electrochem. Soc.* **121,** 1160 (1974).
12. Kelly, J. J., and Vondeling, J. K., *J. Electrochem. Soc.* **122,** 1103 (1975).
13. Dunn, W. W., and Bard, A. J., *Nouv. J. Chim.* **5,** 651 (1981).
14. Stadler, K. H., and Boehm, H. P., *in* "Proceedings, 8th International Congress on Catalysis, Berlin, 1984," Vol. IV, p. 803. Dechema, Frankfurt-am-Main, 1984.
15. Jacobs, J. W. M., *J. Phys. Chem.* **90,** 6507 (1986).
16. Jacobs, J. W. M., and Schryvers, D., *J. Catal.* **103,** 436 (1987).
17. White, J. R., and O'Sullivan, E. J. M., *J. Electrochem. Soc.* **134,** 1133 (1987).
18. Yoneyama, H., Nishimura, N., and Tamura, H., *J. Phys. Chem.* **85,** 268 (1981).
19. Borgarello, E., Harris, R., and Serpone, N., *Nouv. J. Chim.* **9,** 743 (1985).
20. Serpone N., Borgarello, E., Barbeni, M., Pelizzetti, E., Pichat, P., Herrmann, J. M., and Fox, M. A., *J. Photochem.* **36,** 373 (1987).
21. Fleischauer, P. D., Alan Kan, H. K., and Shepherd, J. R., *J. Am. Chem. Soc.* **94,** 283 (1972).
22. Hada, H., Tanemura, H., and Yonezawa, Y., *Bull. Chem. Soc. Jpn.* **51,** 3154 (1978).
23. Hada, H., Yonezawa, Y., and Saikawa, M., *Bull. Chem. Soc. Jpn.* **55,** 2010 (1982).
24. Hada, H., Yonezawa, Y., Ishino, M., and Tanemura, H., *J. Chem. Soc. Faraday Trans. 1* **78,** 2677 (1982).
25. Nishimoto, S., Ohtani, B., Kajiwara, H., and Kagiya, T., *J. Chem. Soc. Faraday Trans. 1* **79,** 2685 (1983).
26. Ohtani, B., Okugawa, Y., Nishimoto, S., and Kagiya, T., *J. Phys. Chem.* **91,** 3550 (1987).
27. Herrmann, J. M., Disdier, J., and Pichat, P., *J. Catal.* **113,** 72 (1988).
28. Serpone, N., Borgarello, E., and Pelizzetti, E., *in* "Photocatalysis and Environment" (Mario Schiavello, Ed.), Series C, Vol. 237, p. 527, Kluwer, Dordrecht, NATO ASI Series.
29. Crucq, A., and Frennet, A., Eds., "Catalysis and Automotive Pollution Control (CAPOC I)," Studies Surf. Sci. Catal., Vol. 30, Elsevier Amsterdam, 1987 and next volume (CAPOC II) to be published in the same series.
30. Fernandez, A., Munuera, G., Gonzalez-Elipe, A. R. Espinos, J. P., Herrmann, J.-M., Pichat, P., and Leclercq, C., *Appl. Catal.* **57,** 191 (1990).
31. Herrmann, J.-M., *J. Catal.* **89,** 404 (1984).
32. Gonzalez-Elipe, A. R., Espinos, J. P., Fernandez, A., and Munuera, G., *J. Catal.*, **130,** 627 (1991).